Proceedings of the
Annual Stability Conference
Structural Stability Research Council
St. Louis, Missouri, April 2-5, 2019

Evaluating Critical Temperatures of Axially Loaded I-shaped Steel Members Using ANSI/AISC-360 Appendix 4 and Finite Element Model

Ana Sauca[1], Chao Zhang[2], Mina Seif[3], Lisa Choe[4]

Abstract
Stability is paramount to the load-carrying capacity of structural steel members subjected to fire. Actual buckling strengths of steel members in fire become lower than that at ambient temperature since modulus of elasticity (E) and yield strength (F_y) significantly diminish with increasing temperatures. Appendix 4 of the ANSI/AISC-360 specification provides an equation for calculating the flexural buckling stress (F_{cr}) of columns at temperatures greater than 200 °C. However, finite element analysis showed that columns can fail by buckling at temperatures below 200 °C if the applied axial load is greater than 80 % of its ambient compressive strength. This paper presents: (i) critical temperatures estimated using both the Appendix 4 equations and finite-element analysis and (ii) parametric study results showing effects of applied load level, member slenderness, and steel grades on the critical buckling temperature. Closed form equations are developed and presented along with limitations for use in design practice.

1. Introduction

The critical temperature method has been considered a useful tool to evaluate failure temperatures of loaded steel members exposed to a standard fire (e.g., ISO-834 (International Standard ISO 834-1:1999)). The Eurocode 3 (EC3) standard (EN 1993-1-2, 2005) specifies the critical temperature method for steel members supporting given axial or flexural loads. This method assumes that a loaded steel member is heated uniformly along its length and across the cross-section. For steel members without any instability phenomenon (e.g., tensile or flexural members) the critical temperature ($\theta_{a,cr}$) can be determined using Eq. (1) which is a function of the degree of utilization (μ_0) in Eq. (2), where ($E_{fi,d}$) is the design effect of actions for the fire design situation; ($R_{fi,d,0}$) is the corresponding design resistance of the steel member for the fire design situation at time (t) = 0.

[1] Guest Researcher, National Institute of Standards and Technology (NIST), <ana.sauca@nist.gov>
[2] Guest Researcher, National Institute of Standards and Technology (NIST), <chao.zhang@nist.gov>
[3] Research Structural Engineer, National Institute of Standards and Technology (NIST), <mina.seif@nist.gov>
[4] Research Structural Engineer, National Institute of Standards and Technology (NIST), <lisa.choe@nist.gov>

$$\theta_{a,cr} = 39.19 ln\left[\frac{1}{0.9674\mu_0{}^{3.833}} - 1\right] + 482 \quad (1)$$

$$\mu_0 = \frac{E_{fi,d}}{R_{fi,d,0}} \quad (2)$$

For steel members prone to instabilities (e.g. columns), the critical temperature is presented in specific tabulated data (Vassart et al., 2014), depending upon the degree of utilization, the steel grade, and the non-dimensional slenderness. The non-dimensional slenderness can be determined using Eq. (3), where (A) is the gross cross-sectional area (for class 1, 2 and 3 cross sections) or the effective area of a cross section (for class 4 cross sections), (F_y) is the yield stress and (N_{cr}) is the elastic critical force for the relevant buckling mode based on the gross cross-sectional properties. In Eurocode 3 (EC3), for class 4 cross sections, the resistance and rotation capacity is limited by their local buckling resistance.

$$\bar{\lambda} = \sqrt{\frac{AF_y}{N_{cr}}} \quad (3)$$

Some national annexes of Eurocodes specify values for critical temperatures. For example, the British Standard (BS NA EN1993-1-2, 2005) provides critical temperatures for columns and beams. When evaluating the beams, the values of specified critical temperatures vary with fire protection, the support conditions of floor slabs, and the degree of utilization. When evaluating columns, the values of specified critical temperatures vary with the non-dimensional slenderness and the degree of utilization.

Appendix 4 of the American Institute of Steel Construction (AISC) specification for structural steel buildings, known as ANSI/AISC-360 (AISC, 2017), provides advanced and simple methods of analyses for fire conditions; however, it omits the critical temperature method. Hence, the objective of this study presented in this paper is to evaluate and compare the critical temperature of axially loaded I-shaped steel members using simple method of analysis specified in ANSI/AISC-360 Appendix 4 and finite-element models. The parameters influencing critical temperatures were evaluated, such as the effects of applied load levels, member slenderness ratios, steel grades, and section compactness. Closed-form equations were developed and presented along with limitations for use in design practice.

2. Critical temperature of steel members using ANSI/AISC-360 Appendix 4

Buckling strengths of steel members subject to fire conditions decrease as the modulus of elasticity (E) and yield strength (F_y) diminish with increasing temperatures. Appendix 4 of ANSI/AISC-360 specifies Eq. (4) for calculating the flexural buckling stress (F_{cr}) at temperatures greater than 200 °C, where ($F_y(T)$) is the yield stress at elevated temperature; ($F_e(T)$) is the critical elastic buckling stress calculated from Eq. (5); ($E(T)$) is the elastic modulus at elevated temperatures; (L_c) is the effective length of member; and (r) is a radius of gyration which is equal to $(I/A)^{0.5}$, where (I) is the area moment of inertia and (A) is the cross-sectional area.

$$F_{cr}(T) = \left[0.42^{\sqrt{\frac{F_y(T)}{F_e(T)}}}\right] F_y(T) \tag{4}$$

$$F_e(T) = \frac{\pi^2 E(T)}{\left(\frac{L_c}{r}\right)^2} \tag{5}$$

Chapter E of ANSI/AISC-360 uses Eq. (6) and Eq. (7) to calculate the flexural buckling stress (F_{cr}) at ambient conditions depending on the value of (L_c/r). In these equations, the yield stress (F_y), the Young's modulus (E), and the critical elastic stress (F_e) are all ambient temperatures values.

When $\frac{L_c}{r} \leq 4.71\sqrt{\frac{E}{F_y}}$ (or $\frac{F_y}{F_e} \leq 2.25$)

$$F_{cr} = \left(0.658^{\frac{F_y}{F_e}}\right) F_y \tag{6}$$

When $\frac{L_c}{r} > 4.71\sqrt{\frac{E}{F_y}}$ (or $\frac{F_y}{F_e} > 2.25$) (7)

$$F_{cr} = 0.877 F_e$$

For columns with compact sections, the nominal compressive strength for flexural buckling at ambient conditions is computed using the flexural buckling stress at ambient conditions (F_{cr}) and the gross cross-sectional area (A) as presented in Eq. (8). For elevated temperatures, Eq. (4) provided in Appendix 4 of the ANSI/AISC-360 replaces Eq. (6) and (7) to calculate the nominal compressive strength for flexural buckling.

$$P_n = F_{cr} A \tag{8}$$

For columns with slender sections, the nominal compressive strengths at ambient conditions is computed using Eq. (9), where (A_e) is the effective areas of the cross section.

$$P_n = F_{cr} A_e \tag{9}$$

In this paper, the critical temperature can be calculated using the equations presented above for the range of parameters presented in Table 1. The utilization factor is defined as the ratio of ($F_{cr}(T)$) in Eq. (4) to (F_{cr}) in Eq. (6) and Eq. (7) regardless of the section width-to-thickness ratios. The columns are considered simply supported.

Table 1. Considered data to evaluate the critical temperature

Section	**Steel**	**Slenderness** $\frac{L_c}{r}$	**Utilization factor** $\frac{F_{cr}(T)}{F_{cr}}$
W 14x22	Grade 36 (F_y=250 MPa)	20 – 200	0.1 – 1
	Grade 50 (F_y=345 MPa)	20 – 200	0.1 – 1
W 14x90	Grade 36 (F_y=250 MPa)	20 - 200	0.1 - 1
	Grade 50 (F_y=345 MPa)	20 - 200	0.1 - 1

Figure 1 presents the calculated critical temperatures of steel columns using ANSI/AISC-360 Appendix 4 as a function of the utilization ratio for various slenderness values. For columns with utilization factors smaller than 0.5, the effect of slenderness on the critical temperature is deemed small. At the same load level (i.e., utilization factor), the standard deviation of critical temperatures for all slenderness levels was less than 5 % of the averaged value. For utilization factors greater than 0.6, the critical temperature varies significantly with the column slenderness levels. Furthermore, for columns with slenderness values greater than 60 (except slenderness values of 160 and 200) and utilization factors greater than 0.6, the critical temperatures fall below 200 °C, which violates the temperature limit specified for use of Eq. (4) and Eq. (5). Hence, there is a need to limit the utilization factor and slenderness to compute critical temperatures using the AISC equations. The steel grade also has a minor impact on the critical temperatures for most of slenderness levels. Some variations in critical temperatures are observed for shorter columns (with slenderness values less than 40) at utilization factors higher than 0.6.

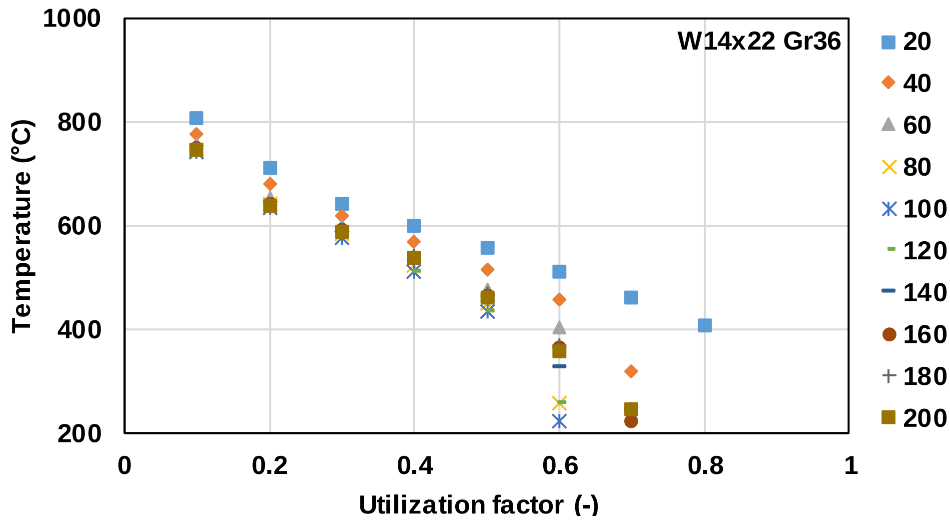

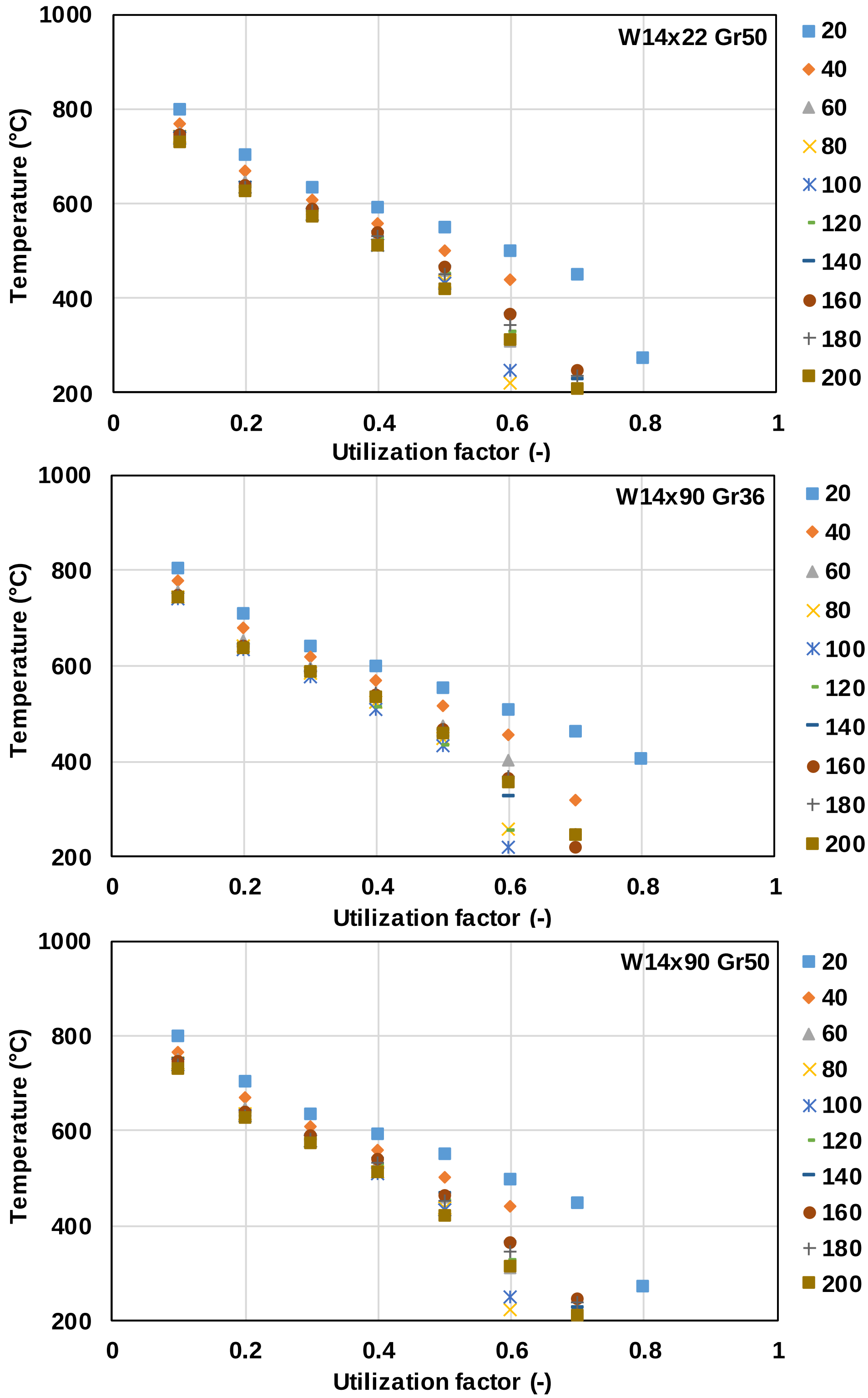

Figure 1. Critical temperature values computed using ANSI/AISC-360 Appendix 4 versus the utilization factor for various slenderness values

3. Critical temperature of steel members using finite element analysis

The cases presented in Table 1 were further evaluated using the finite element analysis software package ANSYS (ANSYS, 2012). The steel column models were meshed with shell element SHELL181, which is a 4-node element with six degrees of freedom at each node. SHELL181 was used because it is suitable for linear, large rotation, and/or large strain nonlinear applications (Index of Software Ansys, 2018), and the change in shell thickness can be accounted for in the nonlinear analysis. The stub and slender columns were meshed using 50 elements for the length, 8 elements for the flange and 8 elements for the web based on the mesh density study presented in Table 2. Linear kinematic constraints were applied to the flanges and web at the column ends to enforce "rigid" planar behavior. At the column ends, the supports were simply supported. Axial force was applied on the center node of the end sections. Global and local initial geometric imperfections were implemented. The initial displacement at midspan was taken as the 1/1000 of the column length to simulate global geometrical imperfections. Local geometrical imperfections were implemented by scaling the deformation of the first (lowest) eigenmode from buckling analysis. The scaled value was the larger of a web out of flatness of ($d/150$) (Kim and Lee, 2002) or a tilt in the compression flanges of ($b_f/150$) (Zhang et al., 2015), where (d) and (b_f) are the height and width of the cross section, respectively. It is noted that for short columns, the local buckling modes are expected to dominate the stability behavior. No residual stresses were applied in the numerical models since the effect is regarded to be rather limited in structural fire analysis (Vila Real et al., 2007). A uniform temperature distribution was assumed through the column cross section and along its length. The EC3 material model was used in this study.

The finite element model of the columns is presented in the Figure 2. Mesh density study presented in Table 2 shows that the relative error for the W14x22 Gr36 section when using the selected mesh is under 2%. Table 3 shows that the relative error for the W14x22 Gr36 section when using the selected time step is under 0.5%.

Table 2. Mesh density study

	Relative error (%) - W14x22 Gr36		
Number of mesh elements (Column Length x Flange x Web)	**Slenderness 20**	**Slenderness 100**	**Slenderness 160**
100 x 16 x 16	-	-	-
50 x 8 x 8 *	-0.20	-1.87	-1.57
30 x 4 x 4	-0.79	-3.53	-9.06

Table 3. Time step influence on the results

	Relative error (%) - W14x22 Gr36
Time step (Initial - Min - Max)	**Slenderness 100**
10 - 0.001 - 100	-0.42
1 - 0.01 – 100 *	-0.42
0.1 - 0.01 - 10	-0.42
0.1 - 0.001 - 1	-

* Selected value in the analysis

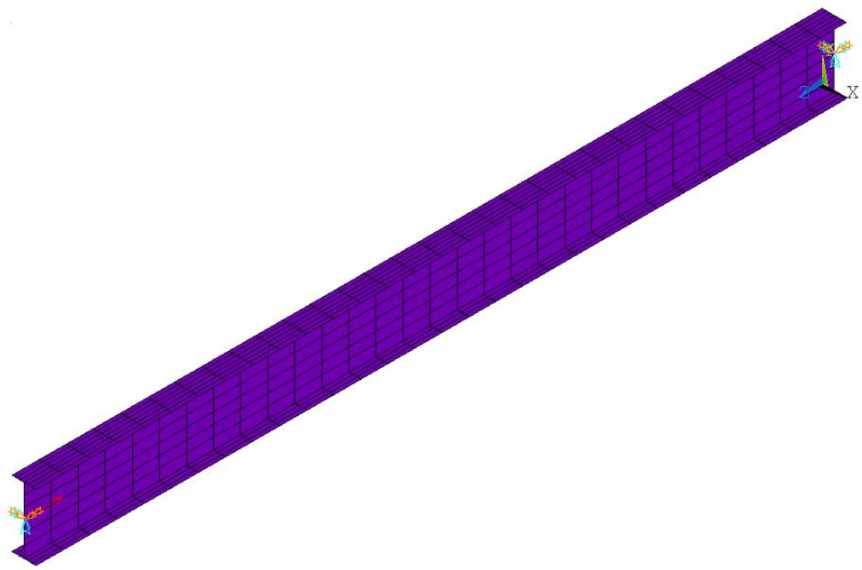

Figure 2. Shell finite element mesh and boundary conditions (ANSYS)

Figure 3 presents the evaluated critical temperatures of steel members using ANSYS versus the utilization ratio for various slenderness values. The critical temperature decreases almost linearly with increasing utilization factors for all slenderness levels. For W14x22 columns, the slenderness has a minor impact on the critical temperature at the same utilization factor. For W14x90 columns, a larger scatter was observed in critical temperatures at utilization factors greater than 0.4.

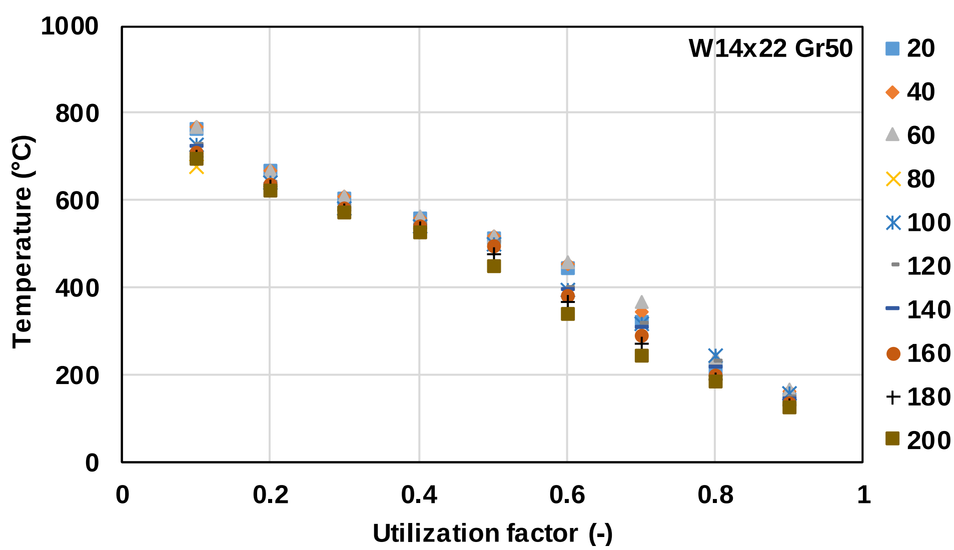

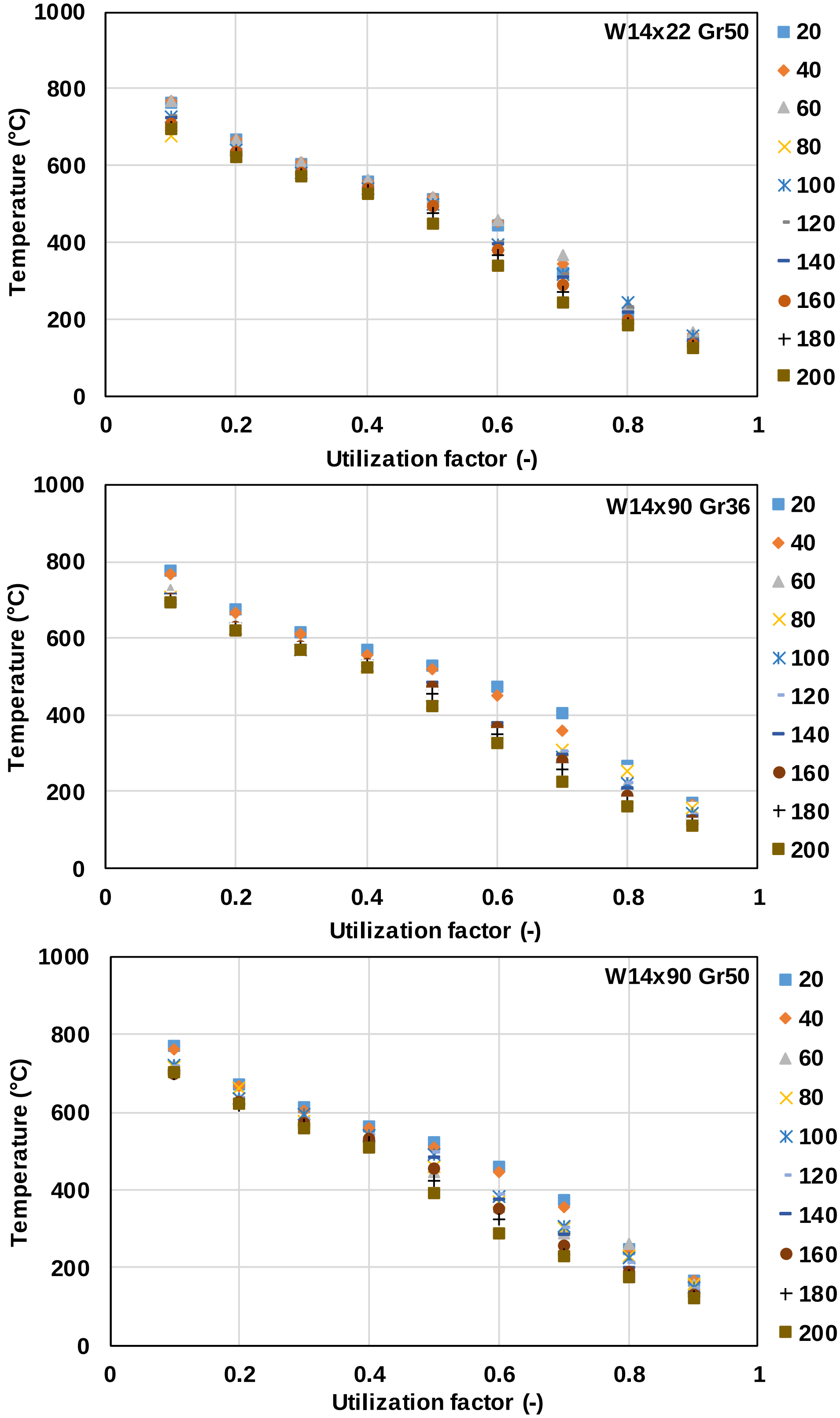

Figure 3. Critical temperature versus the utilization factor for various slenderness values using ANSYS

4. Critical temperatures of steel members using ANSI/AISC-360 Appendix 4 versus finite element analysis

Figure 4 shows a comparison of the computed critical temperatures using ANSI/AISC-360 Appendix 4 versus those computed using ANSYS at practical ranges of utilization factors (0.1 to 0.6) (Moynihan and Allwood, 2014) for slenderness values of 40, 80 and 120. The largest difference between the two methods is as large as 50% for the utilization factor of 0.6. In all the other cases, the temperatures estimated using these two methods are similar (with differences less than 10 %).

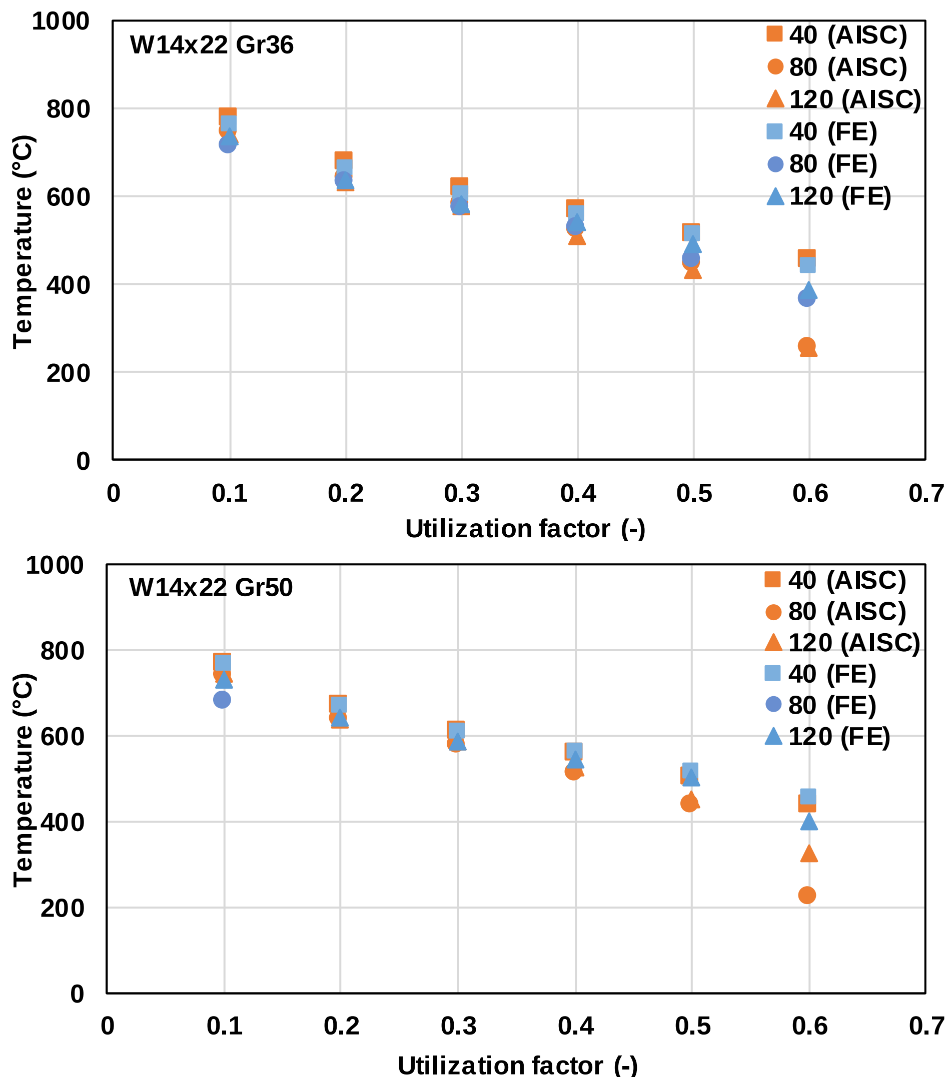

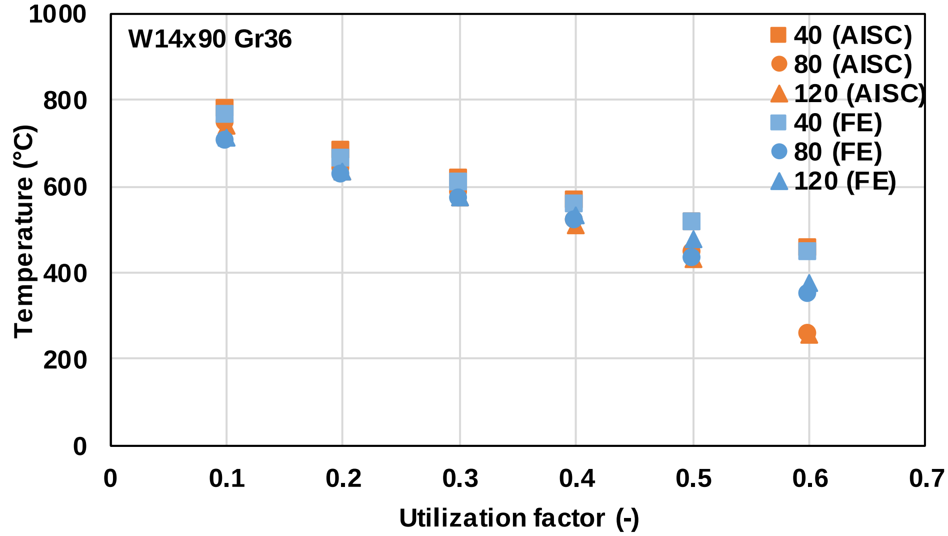

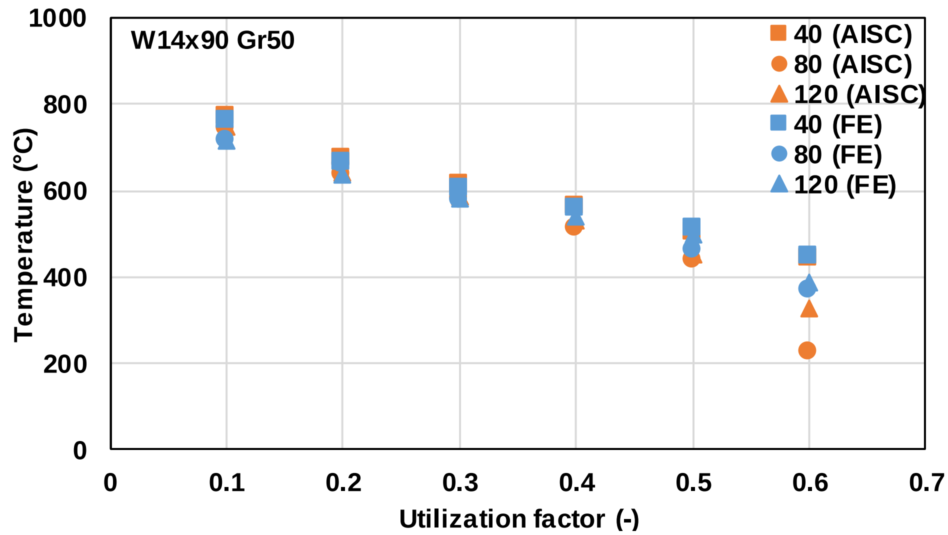

Figure 4: Comparison of critical temperatures versus the utilization factor for slenderness of 40, 80 and 120 based on AISC and ANSYS results

5. Closed formed equation for critical temperature

A closed formed equation for evaluating the critical temperature of steel columns was developed based on the results from the finite element analysis. The considered data were the ones with utilization factors less than 0.6 and temperatures above 400 °C. That is because in practice, (i) the utilization ratio of the columns is between 0.2 and 0.6 (Moynihan, M., C., and Allwood, 2014), and (ii) the degradation of the yield strength of the steel at elevated temperatures starts at 400 °C (Table A-4.2.1 of ANSI/AISC-360).

The critical temperature of steel columns is described in Eq. (10) and is a linear logarithmic function dependent upon the slenderness and the utilization ratio of the columns. The critical temperature equation was determined following the principles presented in the NIST/SEMATECH e-Handbook of Statistical Methods (http://www.itl.nist.gov/div898/handbook/). The standard error, the correlation coefficient (r) and the coefficient of determinations (r^2) are 21.20, 0.97 and 0.95 respectively.

The difference between the critical temperatures estimated using Eq. (10) and the finite element model is below 5% for utilization factors up to 0.4. The maximum difference of 14% occurred at a utilization factor of 0.5 and slenderness of 80.

$$T(°C) = 465.1 + 16.7 ln\frac{r}{L_c} + 150.9 ln\frac{F_{cr}}{F_{cr}(T)} \tag{10}$$

Figure 5 presents the 3D curve fitting of the data.

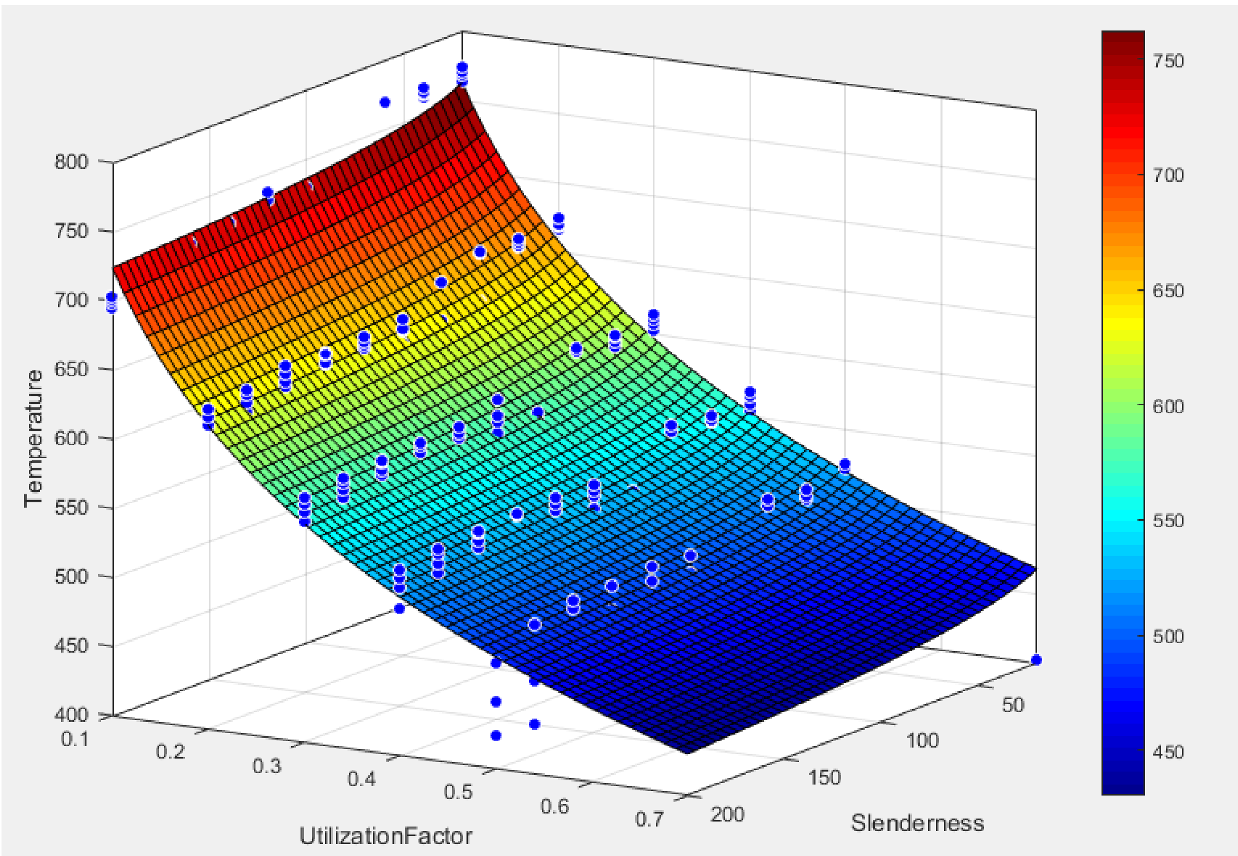

Figure 5: Curve fitting of the data

The proposed equation assumes that all columns cross-sections are uniformly heated, and the boundary conditions are simply supported. The proposed equation was compared with the British National Annex and the results showed differences under 10 %. Ongoing work expands this study, and includes a larger variety of cross-sections, material properties, and boundary conditions.

6. Summary and conclusions

Critical temperatures of steel columns were evaluated using both ANSI/AISC-360 Appendix 4 equations and ANSYS finite element analysis. Both methods yielded similar critical temperatures for utilization ratios less than 0.6. The parametric study shows that for utilization ratios less than 0.6, the impact of member slenderness and steel grades on the critical temperature is deemed small.

For cases with a degree of utilization of 0.6 or higher, however, it is recommended to use finite element analysis. A closed form equation presented in this paper can also be used to estimate the critical temperatures of simply supported steel columns as a function of the member slenderness and the utilization ratio (below 0.6). Future work is needed to evaluate a larger range of section types, of material properties and boundary conditions.

Disclaimer

Certain commercial entities, equipment, products, software, or materials are identified in this paper in order to describe a procedure or concept adequately. Such identification is not intended to imply recommendation or endorsement by the National Institute of Standards and Technology, nor is it intended to imply that the entities, products, software, materials, or equipment are necessarily the best available for the purpose.

References

ANSI/AISC-360 (2017). "Steel Construction Manual". *American Institute of Steel Construction*

ANSYS user manual, version 14.0 ANSYS Inc. (2012)

ASTM E119-18. "Standard Test Methods for Fire Tests of Building Construction Materials". *American National Standard*, West Conshohocken, PA

BS NA EN 1993-1-2 (2005): UK National Annex to Eurocode 3. Design of steel structures. General rules. Structural fire design

EN 1993-1-2 (2005): Eurocode 3: Design of steel structures - Part 1-2: General rules - Structural fire design [Authority: The European Union per Regulation 305/2011, Directive 98/34/EC, Directive 2004/18/EC]

Hyams, D.G. (2018). CurveExpert Professional Documentation. Release 2.6.5

Index of Software Ansys. (Last modified May 2018). Retrieved from https://www.sharcnet.ca/Software/Ansys/16.2.3/en-us/help/ans_elem/Hlp_E_SHELL181.html

International Standard ISO 834-1:1999, Fire Resistance Tests—Elements of Building Construction—Part 1: General Requirements.

Kim S., Lee D. (2002). "Second-order distributed plasticity analysis of space steel frames". *Engineering Structures*, 24 (2002), pp. 735-744

Moynihan, M., C., and Allwood, J., M. (2014). "Utilization of structural steel in buildings". Proc. R. Soc. A 470: 20140170. http://dx.doi.org/10.1098/rspa.2014.0170

NIST/SEMATECH e-Handbook of Statistical Methods, http://www.itl.nist.gov/div898/handbook/, January 31, 2019.

Vassart, O., Zhao, B., Cajot, L.G., Robert, F., Meyer, U., Frangi, A. (2014). "Eurocodes: Background & Applications Structural Fire Design". *JRC Science and Policy Reports*

Vila Real, P.M.M., Lopes da Silva, N.L.S., Franssen, J.M. (2007). "Parametric analysis of the lateral–torsional buckling resistance of steel beams in case of fire". *Fire Safety Journal*, 42 (2007) [461-24]

Zhang, C., Choe, L., Seif, M., Zhang, Z. (2015). "Behavior of axially loaded steel short columns subjected to a localized fire". *Journal of Constructional Steel Research*, 2015; 111:103-111.